JBC RESEARCH ARTICLE

USP10 exacerbates neointima formation by stabilizing Skp2 protein in vascular smooth muscle cells

Received for publication, December 16, 2020, and in revised form, September 14, 2021 Published, Papers in Press, September 29, 2021,
https://doi.org/10.1016/j.jbc.2021.101258

Xiaohong Xia[1,2,‡], Xiaolin Liu[1,‡], Renjie Chai[1,‡], Qiong Xu[1], Zhenyu Luo[1], Jielei Gu[1], Yangshuo Jin[1], Tumei Hu[2], Cuifu Yu[2], Bijun Du[3], Hongbiao Huang[2], Wenchao Ou[1], Shiming Liu[1,*], and Ningning Liu[1,*]

From the [1]Guangdong Key Laboratory of Vascular Diseases, State Key Laboratory of Respiratory Disease, Guangzhou Institute of Cardiovascular Disease, The Second Affiliated Hospital, [2]Guangzhou Municipal and Guangdong Provincial Key Laboratory of Protein Modification and Degradation, School of Basic Medical Sciences, and [3]Department of Obstetrics, The Second Affiliated Hospital, Guangzhou Medical University, Guangzhou, China

Edited by Qi-Qun Tang

The underlying mechanism of neointima formation remains unclear. Ubiquitin-specific peptidase 10 (USP10) is a deubiquitinase that plays a major role in cancer development and progression. However, the function of USP10 in arterial restenosis is unknown. Herein, USP10 expression was detected in mouse arteries and increased after carotid ligation. The inhibition of USP10 exhibited thinner neointima in the model of mouse carotid ligation. *In vitro* data showed that USP10 deficiency reduced proliferation and migration of rat thoracic aorta smooth muscle cells (A7r5) and human aortic smooth muscle cells (HASMCs). Mechanically, USP10 can bind to Skp2 and stabilize its protein level by removing polyubiquitin on Skp2 in the cytoplasm. The overexpression of Skp2 abrogated cell cycle arrest induced by USP10 inhibition. Overall, the current study demonstrated that USP10 is involved in vascular remodeling by directly promoting VSMC proliferation and migration *via* stabilization of Skp2 protein expression.

Cardiovascular diseases are one of the most common causes of death worldwide and mainly arise due to atherogenesis (1, 2). For the treatment of atherogenesis, some surgical procedures, such as stenting, angioplasty, atherectomy, and bypass surgery, are indispensable methods. However, mechanical-injury-induced restenosis is the major threat to the prognosis of these patients (3). A large number of studies have reported that arterial neointima formation is a complicated pathological process caused by vascular smooth muscle cells (VSMCs) dedifferentiation, proliferation, migration, and secretion of extracellular matrix; these are the hallmarks of restenosis (4). The proliferation of VSMCs from the media into the intima leads to neointima formation or intimal hyperplasia. This progression is rare in normal adult arteries in response to stimuli. Notably, VSMC proliferation underlies venous graft failure, the development of postangioplasty restenosis, and transplant arteriosclerosis. Hence, developing strategies targeting VSMC proliferation is essential. Several factors are involved in the progression of VSMC proliferation, but the final common pathway is cell cycle (5). Focus on cell cycle is a promising strategy in patients with surgical procedures.

The different phases of the cell cycle are controlled by a series of protein complexes composed of cyclin-dependent kinase inhibitors and catalytic cyclin-dependent kinases (CDKs) (6). *In vivo* injury or addition of growth factors allows G1/S phase transition *via* activation of CDK complexes (CDK2, CDK4, and CDK6) and downregulating CDKIs (p21, p27, and p57) (6–9). Among these proteins, p27 is a key member of the CKI family that negatively mediates cyclin-CDK holoenzymes in the nucleus to inhibit cell cycle progression at G1/S transition (6). p27 expression is inhibited in the tissue of arterial injury, which is inversely related to VSMC proliferation (9). p27 protein can be polyubiquitinated and degraded by E3 ligases and proteasome (10). Skp2, an F-box component of SCF^{Skp2} ubiquitin ligase, is closely related to and mediates the polyubiquitination of p27 (11). Reportedly, Skp2 is highly expressed in isolated VSMCs. Skp2 deletion in VSMCs inhibits cell proliferation by increasing p27 levels. The latest evidence showed that Skp2 is a direct player in VSMC proliferation *in vivo* to affect the final neointima thickening (12–15).

VSMC plasticity implies rapid change and adaptability through protein turnover. Importantly, the ubiquitin-proteasome system (UPS) plays a critical role in protein turnover, *i.e.*, degradation of proteins related to differentiation, apoptosis, cell-cycle regulation, and signaling (16). UPS also interacts with VSMC proliferation. Inhibiting proteasome remarkably induces VSMC apoptosis and inhibits neointima. The proteasome inhibitors also sensitize VSMC to increased ER stress, triggering cell death (17, 18). Skp2 and CHIP are E3 ligases that enhance VSMC proliferation by regulating p27 and FoxO1 degradation (11, 19, 20). Thus, UPS is a vital effector in VSMC proliferation. However, it contains approximately 100 deubiquitinases (DUBs); whether DUBs have a role in VSMC proliferation is yet elusive. Therefore, in this study, we aimed to investigate whether DUB regulates VSMC proliferation and found that ubiquitin-specific protease 10 (USP10) inhibition reduced VSMC proliferation by promoting Skp2 degradation *in vitro* and *in vivo*.

‡ These authors contributed equally to this work.
* For correspondence: Ningning Liu, liuningning@gzhmu.edu.cn; Shiming Liu, liushiming@gzhmu.edu.cn.

Results

USP10 is increased during artery intimal hyperplasia

Firstly, we performed complete carotid ligation for 21 days. Hematoxylin-eosin (HE) results showed neointima formation in a vascular injury model of artery ligation (Fig. 1*A*). Next, we examined the USP10 level in the carotid. Compared with normal arteries, the level of USP10 was upregulated with complete ligation in carotid arteries. Notably, the expression was more in the neointima than the media in the injured carotid artery. DAPI (blue) represents the expression in the nucleus and α-SMA (green) in the cytoplasm of SMCs. Subsequently, we found that USP10 was located more in the cytoplasm than in the nucleus (Fig. 1*B*). Immunohistochemical analysis indicated that the expression of USP10 was higher in neointima (Fig. 1*C*). These findings suggested that USP10 expression was increased in SMCs during neointima

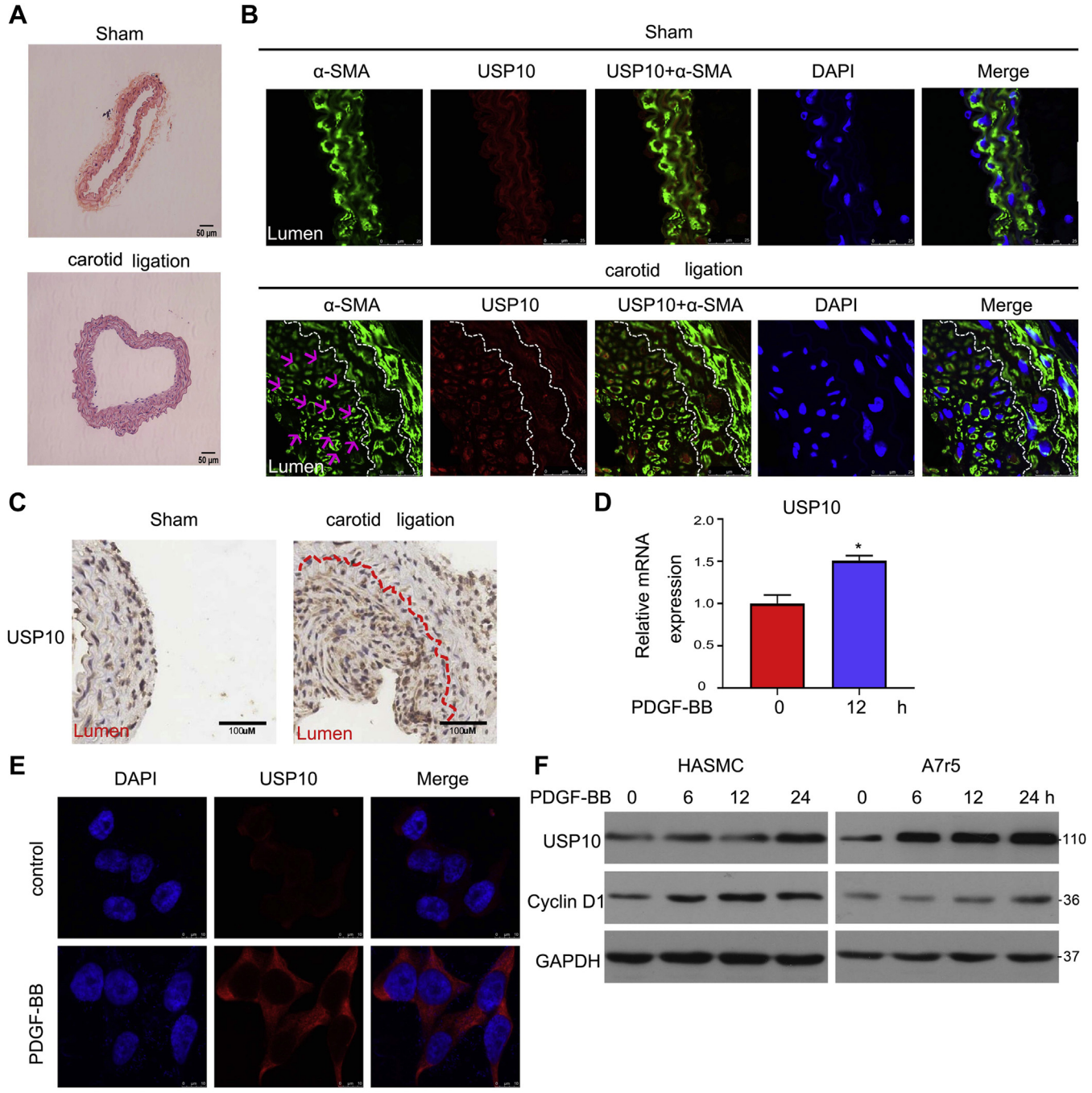

Figure 1. USP10 increases during artery intimal hyperplasia. *A*, representative sections of the carotid arteries from the ligated and sham groups by HE staining. *B*, immunofluorescence staining with USP10 (*red*), DAPI (*blue*), and α-SMA (*green*) in the carotid arteries of sham and ligation groups. *Arrows* (*purple*) represented neointima. *C*, IHC staining with USP10. *D*, HASMCs were treated with PDGF-BB (10 ng/ml) for 12 h, and total RNA was extracted for RT-qPCR to evaluate the USP10 mRNA level. *E*, HASMCs treated with PDGF-BB were subjected to immunofluorescence staining using anti-USP10 antibody, followed by confocal microscopy. *F*, HASMCs and A7r5 cells were treated with PDGF-BB for 0, 6, 12, and 24 h. Total protein was collected to measure USP10 and CyclinD1 expression by Western blot analysis. Representative images are shown. Data are presented as mean ± SD from three independent experiments; $^{*}p < 0.05$.

formation. In addition to the model of carotid ligation, we tested the expression of USP10 in human aortic smooth muscle cell (HASMCs). HASMCs are treated with a potent stimulus of VSMCs (PDGF-BB), and RT-qPCR results showed that USP10 mRNA level was increased after 12 h of stimulation (Fig. 1*D*). Next, we assessed the level of USP10 protein in HASMCs and A7r5 cells and found that it was expressed in the cytoplasm of the mouse carotid tissue and was increased following PDGF-BB stimulation (Fig. 1*E*). The expression of USP10 protein started to upregulate understimulation and remained elevated with prolonged treatment (Fig. 1*F*).

USP10 inhibition or knockdown suppresses VSMCs proliferation in vitro

VSMCs proliferation is a necessary process for neointima formation (21). To detect whether USP10 is involved in VSMCs proliferation, cell viability was assessed using MTS assay in HASMCs and A7r5 cells. USP10 inhibitor (Spautin-1) decreased the viability of VSMCs in a time- and dose-dependent manner (Fig. 2*A*). Moreover, we employed USP10 siRNA to determine cell viability, and the results showed that it was inhibited in HASMCs (Fig. 2, *B* and *C*). Since Spautin-1 affects the activity of USP10 and USP13, we determined whether USP13 is involved in the effect of Spautin-1 in cell viability. MTS assay indicated that USP13 knockdown inhibited cell viability (Fig. S1, *A* and *B*). To investigate the effect of Spautin-1, we knocked down USP13 and combined with Spautin-1 treatment. The results confirmed that USP13 deletion enhanced Spautin-1 induced-cell growth inhibition and Skp2 downregulation, suggesting that the effect of Spautin-1 did not depend on USP13 (Fig. S1, *C* and *D*). Furthermore, PDGF-BB stimuli also promoted cell viability. Under the treatment of PDGF-BB, USP10 inhibition decreased cell viability in VSMCs (Fig. 2*D*). To evaluate the long-term antiproliferation effect of USP10 deletion, colony formation assays were conducted. We found that the cell number of the colony was decreased after USP10 inhibition (Fig. 2, *E* and *F*). Moreover, EdU staining assays showed that USP10 inhibitor-induced DNA replication capacity downregulated with or without PDGF-BB stimuli (Fig. 2, *G* and *H*). Moreover, flow cytometry analysis indicated that USP10 deletion inhibited BrdU incorporation into cells, suggesting that USP10 inhibition/knockdown induced cell proliferation inhibition (Fig. 2, *I*–*L*).

USP10 mediates cell cycle progression and migration in VSMCs

Since USP10 promotes VSMC proliferation, we speculated that it affects cell cycle progression. To investigate whether USP10 mediates cell cycle transition, flow cytometry was employed. As expected, Spautin-1 blocked cell cycle transition from G0/G1 to S phase in HASMCs and A7r5 cells (Figs. 3, *A* and *B* and S2*A*). USP10 knockdown using USP10 siRNA also induced cell cycle arrest (Figs. 3*D* and S2*B*). Additionally, the proteins related to the cell cycle were detected. Western blot assay showed that USP10 inhibitor or siRNA decreased the expression of p-Rb, CDK4, and Cyclin D1 and increased the expression of p27 (Fig. 3, *C* and *E*). Reportedly, VSMC migration plays a critical role in neointima formation (21). However, cell apoptosis could not be affected by USP10 (Fig. 3, *F* and *G*). To examine the effect of USP10 on VSMC migration, we performed scratch and transwell migration assays. The migration of VSMCs was significantly inhibited by USP10 loss (Fig. 3, *H*–*N*). Western blot assay demonstrated that MMP2 was downregulated by Spautin-1, suggesting that USP10 inhibition reduced cell migration (Fig. 3*O*). These findings indicated that USP10 promoted cell proliferation *via* regulation of cell cycle progression and migration in both treatments with and without PDGF-BB but did not trigger cell apoptosis.

USP10 regulates the degradation of Skp2 protein

In a previous study, we reported that as a DUB, USP10 stabilizes Skp2 protein expression in cancer (22). Considering that Skp2 regulates neointima formation, we investigated whether USP10 mediated-VSMC proliferation is regulated by Skp2 expression. Western blot assay showed that Spautin-1 downregulated the level of Skp2 protein in HASMCs and A7r5 cells. Under the treatment of PDGF-BB, Skp2 protein level was increased. In addition, increased PDGF-BB-induced Skp2 was inhibited by Spautin-1 (Fig. 4*A*). The Skp2 expression was also reduced after USP10 knockdown in the treatment with and without PDGF-BB, excluding the off-target effects of Spautin-1 (Fig. 4*B*). Next, we evaluated USP10-induced-Skp2 stability using cycloheximide (CHX). CHX treatment decreased the expression of Skp2 protein in a time-dependent manner. Spautin-1 addition promoted Skp2 protein decrease (Fig. 4, *C* and *D*). In addition to USP10 inhibitor, USP10 siRNA rapidly degraded Skp2 protein, suggesting that USP10 is essential for Skp2 stability (Fig. 4, *E* and *F*).

Interaction between USP10 and Skp2

DUBs regulate their substrate proteins *via* protein–protein interaction and posttranslation. We found that Skp2 protein was regulated by USP10; however, the specific correlations are unknown. Firstly, we used coimmunoprecipitation (Co-IP) assay to detect the interaction between USP10 and Skp2. The results showed that USP10 interacts with Skp2 protein in HASMCs, and Skp2 also binds with USP10 (Fig. 5*A*). Moreover, HEK293T transfected with FLAG-USP10 and MYC-Skp2 were subjected to Co-IP and Western blot assays. We found that exogenic MYC-tagged Skp2 interacted with FLAG-tagged USP10, which confirmed a direct interaction between USP10 and Skp2 protein (Fig. 5*B*). The confocal assay showed that Skp2 was mainly located in the nucleus, while cytoplasm exhibited only a slight expression. Therefore, USP10 was colocalized with Skp2 in the cytoplasm of HASMCs. (Fig. 5*C*). The localization of Skp2 and USP10 was observed in the carotid artery after ligation. Consistently, the colocalization of USP10 and Skp2 was detected in the cytoplasm of the artery tissue (Fig. 5*D*). Next, we hypothesized that USP10 mediates the posttranslation of Skp2. In cancer, USP10 decreased Skp2 ubiquitination, and we assessed the level of poly-ubiquitinated Skp2 using Co-IP assay (22). The results showed that the

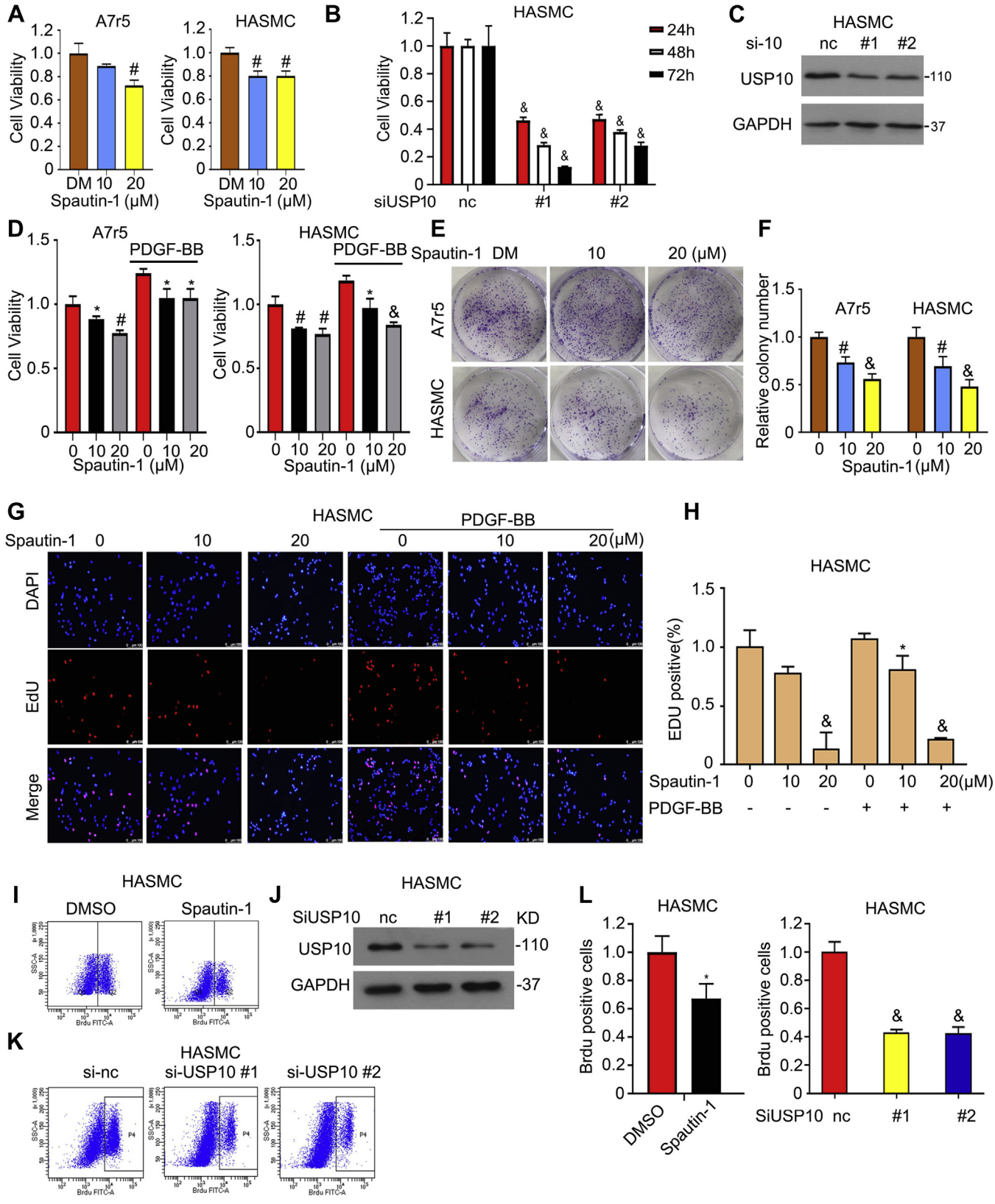

Figure 2. USP10 inhibition or knockdown suppresses VSMC proliferation *in vitro*. *A*, A7r5 cells and HASMCs were treated with Spautin-1 (0, 10, and 20 μM) for 48 h. MTS reagent was added to assess cell viability. *B*, HASMCs were transfected with USP10 siRNA for different time points (24, 48, and 72 h), and MTS assay was performed to assess cell viability. *C*, HASMCs were treated with USP10 siRNA for 48 h, and USP10 expression was assessed by Western blot. *D*, VSMCs were treated with Spautin-1 and PDGF-BB for 48 h, followed by MTS analysis. *E*, VSMCs were treated with Spautin-1 for 48 h, followed by colony formation assay, and *F*, cell number was counted. Representative images are shown. *G*, HASMCs were exposed to Spautin-1 and PDGF-BB and stained with EdU. The images were captured by immunofluorescence microscopy. *H*, the stained cells were counted. *I* and *K*, VSMCs treated with Spautin-1 or siRNA were determined *via* BrdU incorporation assays by flow cytometry. *J*, HASMCs were treated with USP10 siRNA for 48 h, and USP10 expression was assessed by Western blot. *L*, BrdU incorporation was measured. Data are presented as mean ± SD from three independent experiments; $^{*}p < 0.05$, $^{\#}p < 0.01$, $^{\&}p < 0.001$.

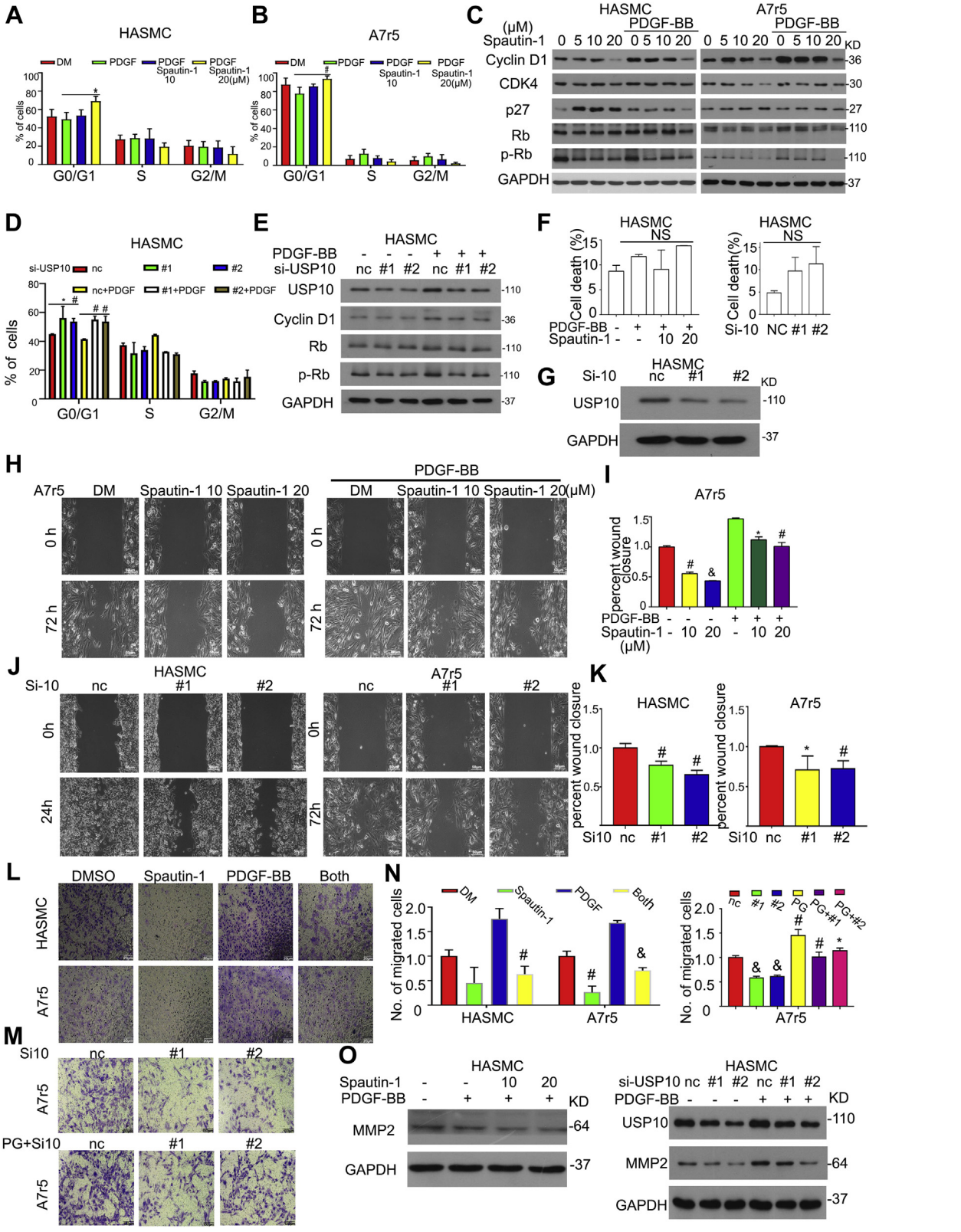

Figure 3. USP10 mediates cell cycle progression and migration in VSMCs. *A*, *B* and *D*, VSMCs were treated with PDGF-BB (10 ng/ml) and Spautin-1 (10 and 20 μM)/USP10 siRNA, or both agents for 48 h. Fluorescence-activated sorting analysis (FACS) was used for cell distribution. *C* and *E*, Western blot assay was performed on VSMCs treated with PDGF-BB, USP10 inhibitor/siRNA, or the combination for 48 h to detect Cyclin D1, CDK4, p27, p-Rb, and Rb expression. *F* and *G*, HASMCs were treated with PDGF-BB, and PDGF-BB+Spautin-1/USP10 siRNA, followed by flow cytometry analysis and Western blot to test cell apoptosis and USP10 expression. *H–K*, wound healing assay was performed on VSMCs treated with Spautin-1/USP10 siRNA or PDGF-BB+Spautin-1/USP10 siRNA. *L–N*, transwell migration assay was performed on VSMCs exposed to Spautin-1/USP10 siRNA, PDGF-BB, or the combination of both treatments. *O*, same treated cells were subjected to Western blot to assess MMP2 expression. GAPDH served as the loading control.

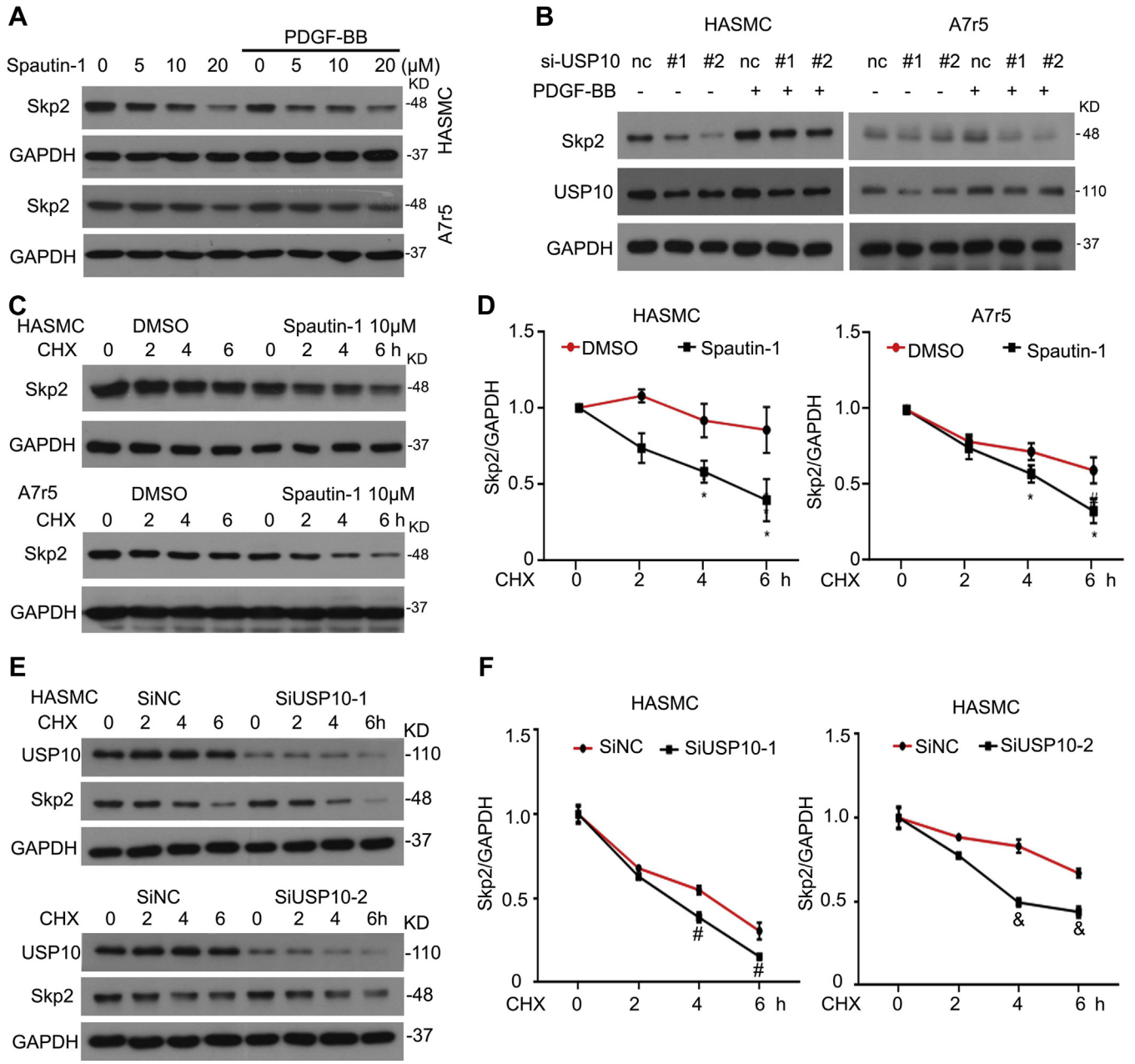

Figure 4. USP10 regulates the degradation of Skp2 protein. *A*, VSMCs were exposed to Spautin-1 (0, 5, 10, and 20 μM) or PDGF-BB was added for 48 h, followed by Western blot analysis for Skp2 expression. *B*, HASMCs and A7r5 cells were transfected with USP10 siRNA or PDGF-BB+USP10 siRNA for 48 h, and Skp2 and USP10 protein expression was assessed. *C*, VSMCs were pretreated with Spautin-1 for 24 h and exposed to CHX (50 μg/ml) for 0, 2, 4, and 6 h. The extracted protein using western blot analysis for Skp2 expression. *D*, the band of Skp2 was assessed using image J. *E*, HASMCs were transfected with USP10 siRNA for 48 h and then treated with CHX for 0, 2, 4, and 6 h. *F*, Skp2 expression was calculated based on Western blot analysis. GAPDH served as the loading control. Data are presented as mean ± SD from three independent experiments. $^{*}p < 0.05$, $^{\#}p < 0.01$, $^{\&}p < 0.001$.

inhibition or silencing of USP10 increased the level of ubiquitinated Skp2 remarkably (Fig. 5, *E* and *F*).

Skp2 overexpression abrogates USP10 deletion-induced events

USP10 had a proproliferative effect on VSMCs and stabilized Skp2 protein expression. To study the regulatory mechanism of USP10 on VSMCs, we tested the effects of USP10 and Skp2 on cell growth and found that USP10 overexpression using lentivirus containing human USP10 induced G0/G1 to S phase progression (Figs. 6*A* and S3*A*). Western blot assay assessed the proteins associated with cell cycle. Cyclin-dependent kinase inhibitor, p27, was decreased, and Skp2 expression was increased by overexpressing USP10 in HASMCs (Fig. 6*B*). In addition, lentivirus containing human Skp2 was employed to transfect HASMCs, followed by MTS and colony formation analysis. The results showed that overexpression of Skp2 promoted cell proliferation (Fig. 6, *C–E*). To determine whether USP10-induced the biological effect

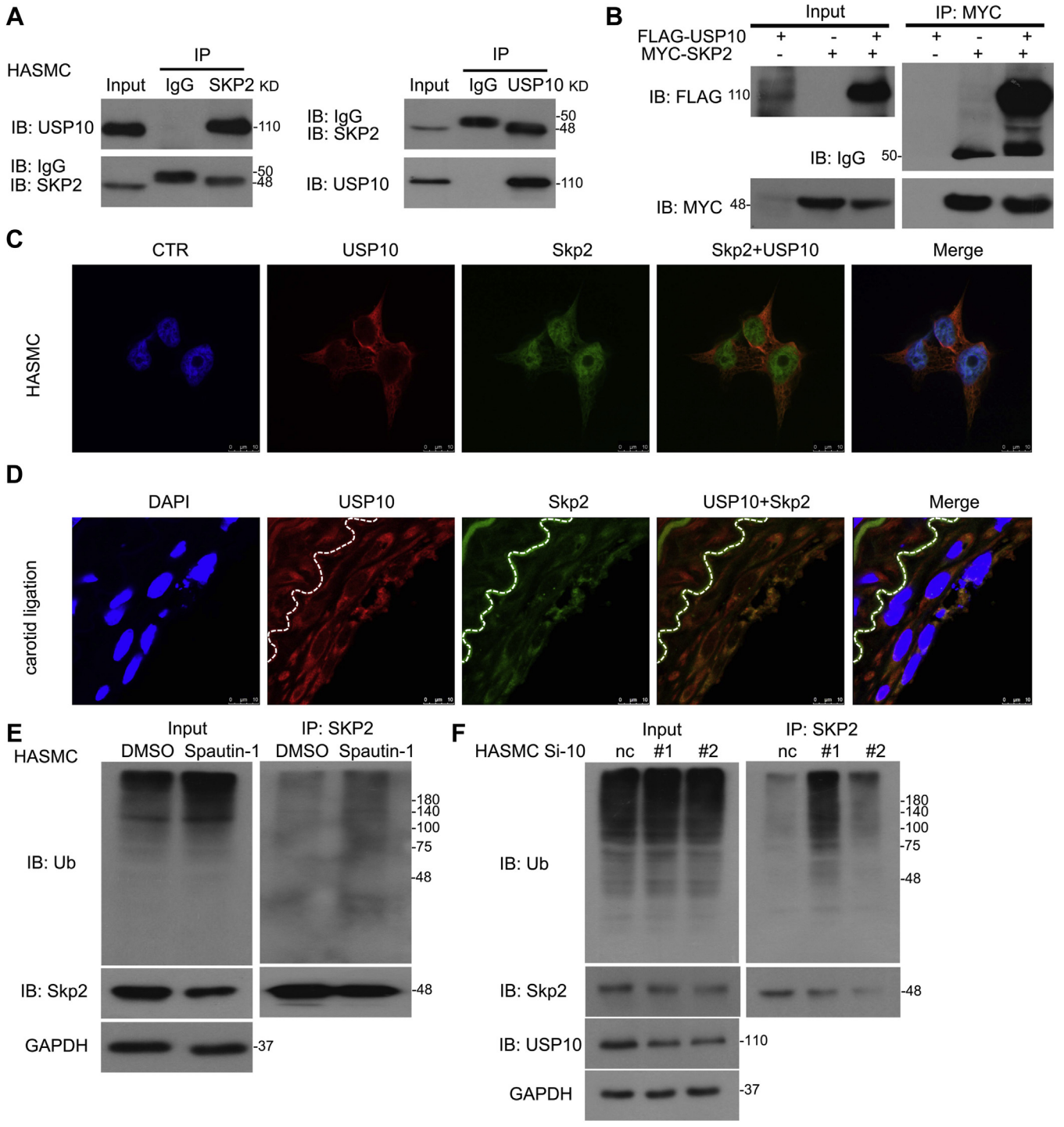

Figure 5. Interaction between USP10 and Skp2. *A*, protein was collected from HASMCs. After immunoprecipitation with Skp2 or USP10, the proteins were assessed by immunoblotting. *B*, HEK293T cells were transfected with FLAG-tagged USP10 and MYC-tagged Skp2 for 48 h. After immunoprecipitation with MYC, immunoblotting was carried out with FLAG and MYC. *C*, HASMCs were transfected with lentivirus overexpressing Skp2 and USP10 for 48 h and then incubated with anti-Skp2 and anti-USP10 antibodies. The images were captured by fluorescence microscopy. *D*, carotid arteries with ligation were incubated with anti-USP10 and anti-Skp2 antibodies, followed by fluorescence microscopy. *E*, cells were treated with Spautin-1 (10 μM), immunoprecipitated with Skp2, and immunoblotted with Ub and Skp2. *F*, cells were transfected with USP10 siRNA (50 nM) for 48 h, immunoprecipitated with Skp2, and immunoblotted with Ub and Skp2.

depended on Skp2 status, HASMCs were transfected with lentivirus containing human Skp2 and then treated with USP10 inhibitor (Spautin-1). Skp2 overexpression abrogated the cells from USP10 inhibition-triggered G1 arrest. The altered p27 and Cyclin D1 proteins were rescued after overexpressing Skp2 (Figs. 6, *F* and *G* and S3*B*). Meanwhile, Skp2 rescued USP10 siRNA induced-cell cycle arrest. (Figs. 6, *H* and *I* and S3*C*).

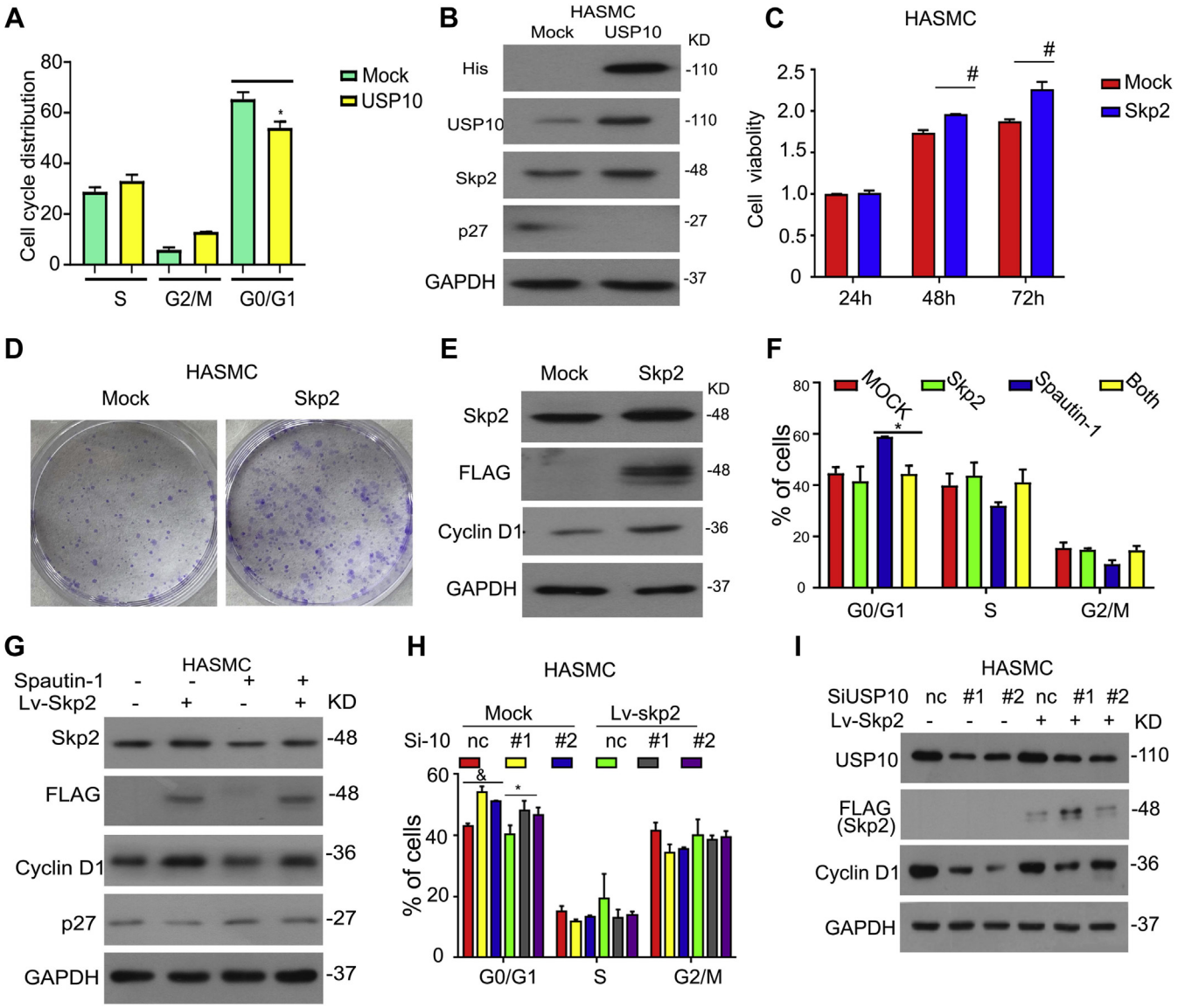

Figure 6. Skp2 overexpression abrogates USP10 deletion-induced events. *A*, HASMCs were transfected with lentivirus containing human USP10 for 48 h, followed by FACS. *B*, protein was extracted and subjected to Western blot analysis for related protein expression. *C* and *D*, HASMCs were transfected with lentivirus containing human Skp2 for 48 h, followed by MTS and colony formation assays. *E*, protein was extracted, and Western blot assay was performed to evaluate Skp2, FLAG, and Cyclin D1 proteins. *F* and *H*, HASMCs were transfected with lentivirus containing human Skp2 and Spautin-1/USP10 siRNA, followed by FACS. *G* and *I*, total protein was extracted and Western blot assay was performed to evaluate Skp2, FLAG, Cyclin D1, and p27 proteins. GAPDH served as the loading control.

Spautin-1 inhibits neointima formation

USP10 was upregulated in VSMCs after carotid ligation, and whether USP10 is a promotor in neointima formation under vascular injury was elucidated. Thus, we established the mice model of carotid ligation. USP10 inhibitor (Spautin-1) was employed to treat the mice. As shown in Figure 7*A*, USP10 inhibition significantly decreased neointima formation and reduced intima/media rations (Fig. 7*B*). In addition, we observed that their vitality was influenced by blood pressure (BP) and heart rate, which were associated with vascular remodeling but did not differ markedly. The body weight was also similar between the control and treatment groups after 3-week complete carotid ligation (Fig. 7*C*). Immunohistochemistry (IHC) results showed that USP10 inhibition inhibited Skp2 expression in the model of carotid ligation. Also, USP10 ablation in SMCs decreased injury-induced upregulation of MMP2 (Fig. 7*D*). Collectively, these data suggested that USP10 plays a role during restenosis. To further investigate the effect of USP10, we applied EGFP-tagged AAV-USP10 shRNA to knockdown USP10 expression *in vivo*. Immunofluorescence analysis demonstrated the success of USP10 deletion in mice (Fig. 7, *E* and *F*). Intima areas indicated that USP10 deficiency inhibited neointimal formation (Fig. 7, *G* and *H*); however, no significant difference was detected between the two groups (Fig. 7*I*).

Discussion

Neointima formation commonly occurs during vein bypass graft failure, arterial restenosis development, and atherosclerosis (5). However, the underlying molecular mechanisms

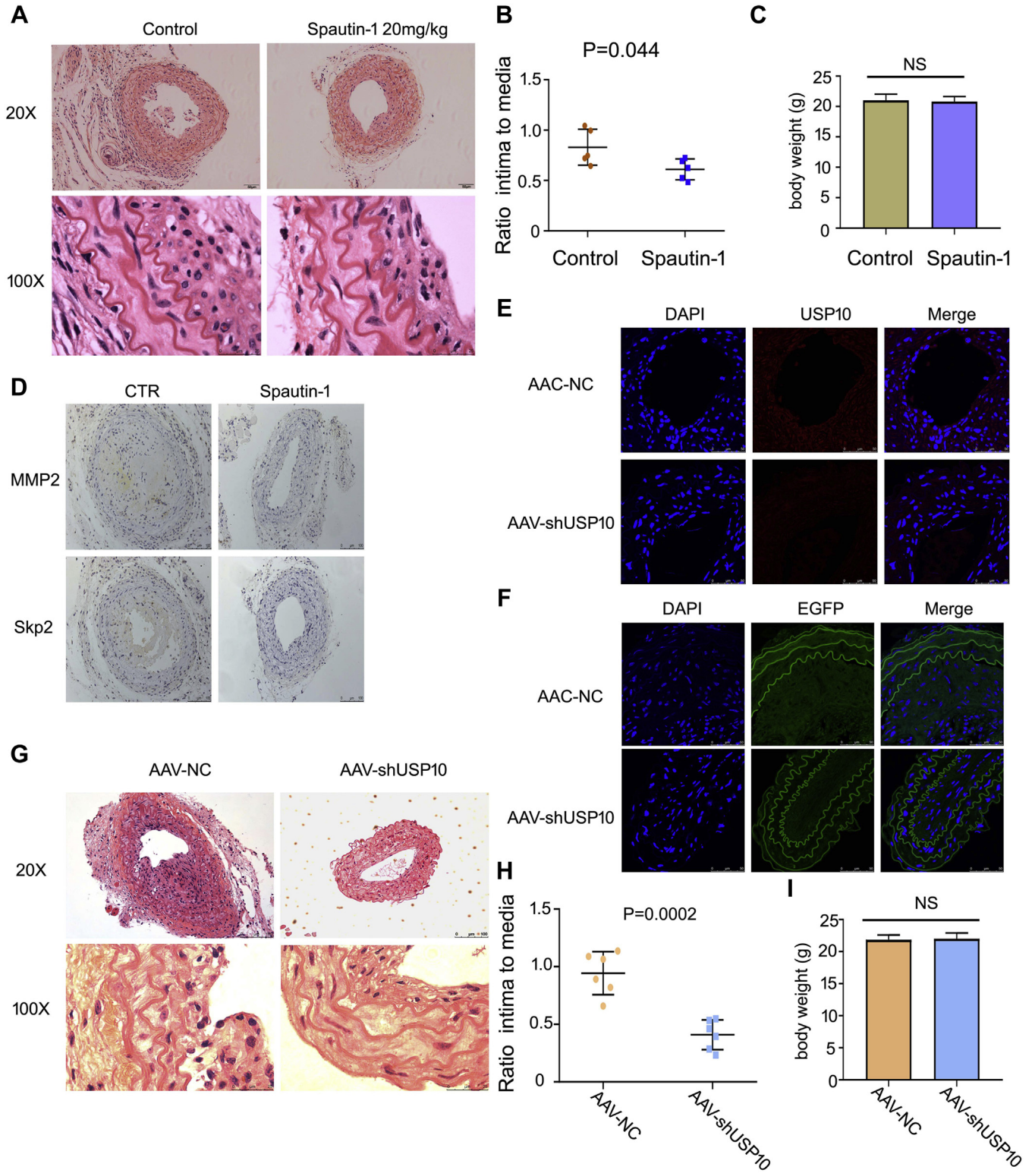

Figure 7. Spautin-1 inhibits neointima formation. *A*, representative images of HE-stained ligated carotid artery from C57BL mice after 3-week carotid ligation (n = 5/group). *B*, student's *t* test was applied to compare the two groups. *C*, body weight is shown. *D*, Skp2 and MMP2 expression was tested using IHC analysis. Immunofluorescence staining with anti-USP10 (*red*) (*E*) and anti-EGFP (*green*) (*F*) in the carotid arteries of sham and ligation groups. *G*, representative images of HE-stained ligated carotid artery from C57BL mice (n = 6/group). *H*, student's *t* test was applied to compare two groups. *I*, body weight is presented.

remain to be elucidated in this complicated pathophysiological progress. In this study, we identified USP10-Skp2 axis and investigated the role of USP10 in vascular remodeling. USP10 expression was highly expressed in the carotid artery of intimal hyperplasia compared with the normal carotid artery. Skp2 was essential for USP10-induced vascular proliferative

pathology. These findings indicated a critical role of USP10 in orchestrating a complex pathological process of vascular restenosis (Fig. 8).

Since its discovery, ubiquitin-specific peptidase 10 (USP10) has been explored primarily in the UPS system with respect to its deubiquitinase activity in cancer progression (23–25). The UPS has been reported to directly or indirectly influence the cellular effects. The UPS-mediated redox and endoplasmic reticulum (ER) homeostasis are strongly related to atherosclerosis. The inhibition of proteasome- or ubiquitin ligase-controlled cell cycle prevents the modulation of the synthetic phenotype, promotes cell apoptosis, and reduces VSMC proliferation and neointima. Over the past decade, the role of protein degradation by UPS gained further support in regulating the transition from contractile to proliferative smooth muscle cell phenotype. Several E3-ligases, Skp2, CHIP, and β-Trcp, regulate VSMC function *via* promoting protein degradation (11, 20, 26). However, DUBs play key roles in the progress of protein degradation. Next, we explored whether there is DUB involved in vascular remodeling. In a recent study, we showed that USP10 triggered the proliferation in chronic myeloid leukemia. Surprisingly, we also identified that USP10 regulated VSMC proliferation. While exploring the effect and expression of USP10 in VSMCs, we used α-SMA as a marker for the identification of SMCs. The gene is expressed in adult SMCs and is considered a classic marker for the recognition of differentiated SMCs (27–29), although it is also expressed in non-SMCs under specific conditions (30). During vascular ligation, USP10 expression increases in VSMCs, which promotes VSMC proliferation and intimal hyperplasia. Moreover, we found that USP10 located in the newly formed intima in the cytoplasm colocalized with α-SMA. In the model of carotid ligation, inhibition of USP10 reduced the intimal hyperplasia. The current results strongly suggested that USP10 is a key promotor in neointima formation.

VSMCs proliferation and migration are critical steps in intimal hyperplasia. As a consequence to arterial injury, endothelium-derived growth-inhibiting factors are downregulated, resulting from endothelial damage, accompanied by platelet activation (31, 32). Subsequently, growth-promoting factors, PDGF products, and VSMCs are elevated (33). PDGF-BB induces VSMC proliferation. *In vitro*, we discovered that USP10 was increased at mRNA and protein levels under PDGF-BB stimuli. The inhibition or knockdown of USP10 decreased the cell viability by blocking the cell cycle transition from G1 to S phase in VSMCs. The cycle protein regulators, such as CDK4, p-Rb/Rb, and p27, were affected by USP10. Additionally, VSMC migration was inhibited by USP10 deletion with or without PDGF-BB stimuli. Importantly, in the molecular mechanism of USP10-regulated cell proliferation, Skp2 was recognized as a target of USP10. Thus, silencing USP10 promoted the degradation of Skp2 protein by increasing its ubiquitination. The protein rescued the events

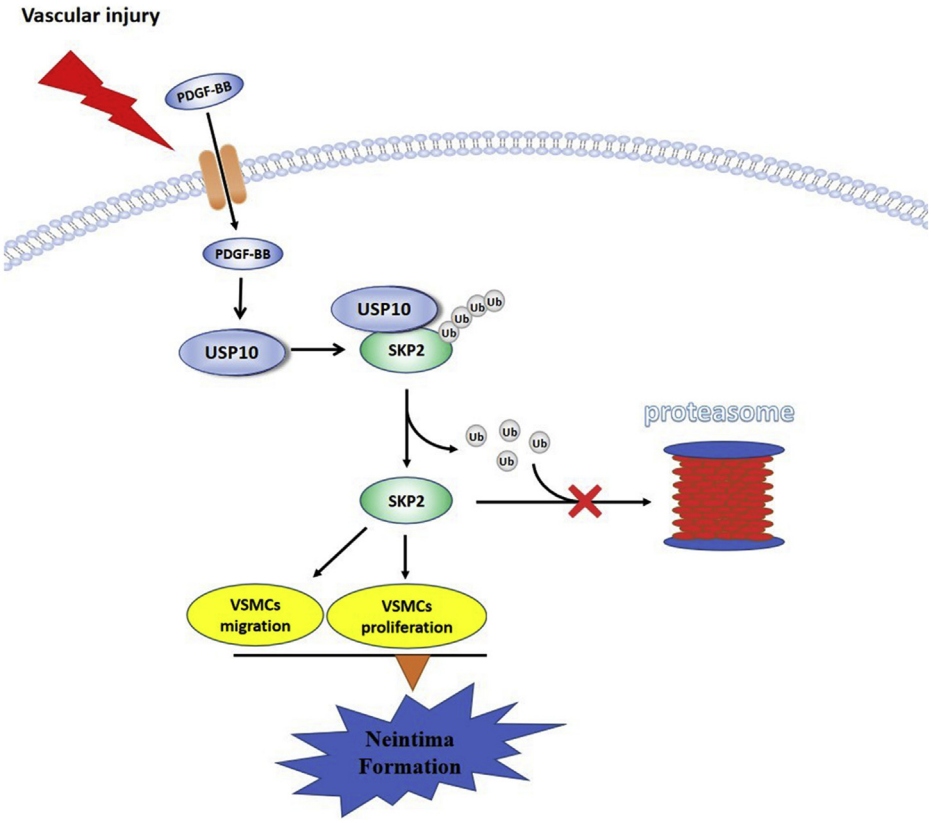

Figure 8. Proposed model of intimal hyperplasia regulated by USP10. This finding demonstrated the role of USP10 in intimal hyperplasia. USP10 expression was increased in ligated carotid and under PDGF-BB stimuli. USP10 interacts with Skp2 and suppresses its degradation by ubiquitination. USP10 loss inhibits VSMC proliferation and neointima formation by downregulating Skp2 expression.

induced by USP10 inhibition. The findings indicated that Skp2 was involved in the progression of USP10-promoted VSMC proliferation.

Taken together, this study demonstrated a major role of USP10 in neointima formation and established it as a deubiquitinating enzyme of Skp2 in VSMCs *via* interaction with Skp2 and removal of ubiquitin.

Experimental procedures

Materials

Spautin-1 (S7888) and cycloheximide (S7418) were obtained from Selleckchem. Antibodies, anti-USP10 (#8501), anti-Skp2 (#2652), anti-p-Rb (#8516), anti-Rb (#9309), anti-CDK4 (#12790), anti-Cyclin D1 (#55506), anti-p27 (#3686), anti-MMP2 (#40994), anti-ubiquitin (#3936), anti-α-SMA (#19245), and anti-GAPDH (#5174) were purchased from Cell Signaling Technology (CST). Human PDGF-BB was obtained from Peprotech.

Cell culture

HASMCs were purchased from ScienCell, and A7r5 cells were obtained from the Cell Bank of Type Culture Collection of Chinese Academy of Sciences. Cell lines were cultured in DMEM medium containing 10% fetal bovine serum (FBS) at 37 °C containing 5% CO_2.

Cell proliferation analysis and apoptosis assay

In order to assess cell proliferation, we utilized the following assays: cell viability, colony formation, EDU staining, and cell cycle. These assays were performed as described previously (34). Cell viability was tested by MTS (Promega) assay. Briefly, VSMCs were plated into 96-well plates. After 24 h, the indicated reagents were applied to treat the adherent cells. A volume of 20 μl MTS was added to the well and incubated for 3 h. The cell viability was evaluated based on the absorbance of optical density. The cells were seeded into 6 cm dishes and treated at the indicated concentrations. The treated cells were digested and transferred to 6-well plate for culture for 10 to 14 days. Then, the cells were washed with phosphate-buffered saline (PBS), fixed with 4% paraformaldehyde for 10 min, and stained with 1% crystal violet solution.

EdU staining was carried out to recognize replicating DNA. The kit was obtained from Ribobio. VSMCs were plated into chamber slider and treated with Spautin-1 and PDGF-BB for 48 h and then 50 μM EdU for 2 h. Subsequently, glycine and 0.5% Triton X-100, Apollo reaction cocktail, and DAPI were applied successively for 5, 10, 30, and 5 min, respectively. The images were captured by the Olympus microscope. For cell cycle assay, the cells were plated, treated, washed with PBS, resuspended in 2 ml of 70% ethanol and 500 μl PBS at 4 °C for one night. The cells were then stained with propidium iodide (PI), RNase A, and 0.2% Triton X-100 for half an hour. The cell distribution was tested by flow cytometry. Cell apoptosis assay was performed using Annexin V-FITC/PI kit (Cat.# KGA108). The treated cells were washed with PBS and stained for 15 min before flow cytometry was used to analyze cell apoptosis.

Scratch and transwell assays

For measuring the cell migration activity, we used scratch and transwell assays. To perform scratch assay, cells were seeded into 6-well plates and treated with Spautin-1. When the cells were cultured to 90% confluency, a 200 μl pipette tip was used to scrape the cell monolayer to make a wound. The images were acquired digitally at 0 and 72 h using an inverted Olympus microscope. For transwell assay, the treated cells were suspended in a serum-free medium and seeded into the upper chamber. The lower chamber was supplemented with 600 μl of 10% FBS medium. After the indicated time point, the transwell was fixed with 4% paraformaldehyde for 10 min and then stained with 1% crystal violet.

Western blot assay

This assay was carried out as described previously (35). The cells were treated as indicated, and proteins were extracted with RIPA buffer and protease inhibitors (CST). The BCA kit was utilized to estimate the protein concentration. An equivalent of protein was separated by 12% SDS-PAGE and transferred to polyvinylidene difluoride (PVDF) membrane for 2.5 h. Then, the membranes were blocked using 5% milk in PBS-T and probed with primary and secondary antibodies for the indicated time points. Finally, an ECL detection kit was used to develop the immunoreactive bands, and the membrane was exposed to X-ray films (Kodak).

Co-IP analysis

This assay was performed as described previously (36). Briefly, antibody and Dynabeads (Invitrogen) were mixed in a reaction for 16 to 24 h. The extracted proteins were mixed with the Dynabeads carrying antibody and incubated for 1 h. The protein was separated from the Dynabeads *via* centrifugation and evaluated by Western blot analysis.

Immunofluorescence assay

This assay was performed as described previously (37). The treated cells were washed with PBS and fixed with 4% paraformaldehyde. Then, the cells were washed with PBS, followed by permeabilization with 0.5% Triton-X for 5 min and blocking with 5% bovine serum albumin (Sigma). Subsequently, the cells were incubated with a primary antibody at 4 °C and anti-IgG H&L (mouse or rabbit) secondary antibody for 1 h. DAPI was used for nuclear staining, and images were captured by a confocal microscope (Leica TCS SP8). Mouse carotid artery tissues were sliced into 5-μm-thick sections at the optimal cutting temperature and incubated with anti-USP10 (NBP2-01452, Novus Biological, 1:100), anti-α-smooth muscle actin (α-SMA, ab7817, Abcam, 1:200), and anti-Skp2 (15010-1-AP, Proteintech, 1:50), respectively.

Plasmid and RNA transfection

The plasmids in this study (Flag-USP10 and Myc-Skp2) were purchased from GeneChem. This assay was performed

as reported previously (38). The adherent cells were incubated in a mixture containing RPMI opti-MEM (Gibco), P3000, plasmids, and Lipofectamine 3000 for 15 min. After 6 h, fresh medium was replaced for an additional 48 h. Furthermore, siRNA (Santa Cruz) was employed to silence the targeted gene. Briefly, the cells were seeded into plates or dishes for 24 h. The mixture containing RPMI opti-MEM, Lipofectamine RNAiMAX, and siRNA was incubated for 15 min and added to adherent cells for 48 h.

Animal models

C57BL/6 female mice were provided for this experiment and approved by the Institutional Animal Care and Use Committee of Guangzhou Medical University. The mice were divided into three groups: sham, control, and treatment. Briefly, a third of the animals were treated with intraperitoneal injection of Spautin-1 (20 mg/kg) or adeno-associated virus by intravenous injection. After 3 days, mice were anesthetized with chloral hydrate, and then the left common carotids proximal to the carotid bifurcation were ligated using 6-0 silk. A similar procedure was performed as control with hydration medium. The sham was not ligated. After 21 days, animals were anesthetized, and the carotid arteries were excised and embedded in paraffin. The carotid arteries were sectioned for HE staining.

Morphology and IHC staining

The carotid sample was collected and fixed with 4% paraformaldehyde overnight. The samples were embedded in paraffin blocks, sliced into 5-μm-thick sections, and subjected to HE staining. For IHC staining, samples were subjected to microwave-based antigen retrieval in 10 mM sodium citrate buffer. Then, 0.3% hydrogen peroxide was applied to inactivate the endogenous peroxide activity for 10 min. Sections were washed with PBS three times, followed by incubation with primary antibodies and secondary antibodies. A standard ABC-peroxidase system and DAB peroxidase substrate kit were used to evaluate the staining intensity.

Generation of overexpressing cell lines

Lentivirus overexpressing Skp2, USP10, or containing control vector was purchased from GeneChem. Cells were seeded into 6-well plates for 24 h. The mixture of polybrene, lentiviruses, and medium was added to cells for 48 h for subsequent analyses.

Statistical analysis

The data are presented as mean ± standard deviation (SD) from three independent experiments. Unpaired Student's t test or one-way analysis of variance (ANOVA) was used to estimate the statistical probabilities where appropriate. GraphPad Prism 8.0 and SPSS 16.0 were used for statistical analysis. $p < 0.05$ indicated statistical significance.

Data availability

All the data and material supporting the conclusions were included in the main paper.

Supporting information—This article contains supporting information.

Acknowledgments—We thank Guangdong Provincial Key Laboratory of Malignant Tumor Epigenetics and Gene Regulation, Sun Yat-Sen Memorial Hospital, Sun Yat-Sen University for flow cytometry analysis. The study was supported by the National Natural Science Foundation of China (82170416, 81873474, 81570259), the Natural Science Foundation of Guangdong (2021A1515011387), the Science and Technology Program of Guangzhou (202002030344), Bureau of Education of Guangzhou Municipality (14CXY03), Guangzhou health and family planning science and technology project (20201A011082), the Key Medical Disciplines and Specialties Program of Guangzhou (2021–2023).

Author contributions—X. X., X. L., R. C., Q. X., Z. L., J. G., Y. J., T. H., C. Y., B. D., H. H., W. O., S. L., and N. L. conceptualization; X. X., X. L., R. C., Q. X., Z. L., J. G., Y. J., T. H., C. Y., B. D., H. H., W. O., S. L., and N. L. data curation; S. L. and N. L. funding acquisition; X. X., X. L., R. C., Q. X., Z. L., J. G., Y. J., T. H., C. Y., B. D., H. H., W. O., S. L., and N. L. methodology; S. L. and N. L. supervision; X. X., S. L., and N. L. writing—original draft; S. L. and N. L. writing—review and editing.

Conflict of interest—The authors declare that they have no conflicts of interest with the contents of this article.

Abbreviations—The abbreviations used are: CDK, cyclin-dependent kinase; CHX, cycloheximide; Co-IP, coimmunoprecipitation; DUB, deubiquitinase; HASMC, human aortic smooth muscle cell; HE, hematoxylin-eosin; IHC, immunohistochemistry; UPS, ubiquitin-proteasome system; USP10, ubiquitin-specific peptidase 10; VSMC, vascular smooth muscle cell.

References

1. Cannon, B. (2013) Cardiovascular disease: Biochemistry to behaviour. *Nature* **493**, S2–S3
2. Glass, C. K., and Witztum, J. L. (2001) Atherosclerosis. The road ahead. *Cell* **104**, 503–516
3. Weintraub, W. S. (2007) The pathophysiology and burden of restenosis. *Am. J. Cardiol.* **100**, 3K–9K
4. O' Brien, E. R., Ma, X., Simard, T., Pourdjabbar, A., and Hibbert, B. (2011) Pathogenesis of neointima formation following vascular injury. *Cardiovasc. Hematol. Disord. Drug Targets* **11**, 30–39
5. Dzau, V. J., Braun-Dullaeus, R. C., and Sedding, D. G. (2002) Vascular proliferation and atherosclerosis: New perspectives and therapeutic strategies. *Nat. Med.* **8**, 1249–1256
6. Tanner, F. C., Yang, Z. Y., Duckers, E., Gordon, D., Nabel, G. J., and Nabel, E. G. (1998) Expression of cyclin-dependent kinase inhibitors in vascular disease. *Circ. Res.* **82**, 396–403
7. Chen, D., Krasinski, K., Sylvester, A., Chen, J., Nisen, P. D., and Andres, V. (1997) Downregulation of cyclin-dependent kinase 2 activity and cyclin A promoter activity in vascular smooth muscle cells by p27(KIP1), an inhibitor of neointima formation in the rat carotid artery. *J. Clin. Invest.* **99**, 2334–2341
8. Izzard, T. D., Taylor, C., Birkett, S. D., Jackson, C. L., and Newby, A. C. (2002) Mechanisms underlying maintenance of smooth muscle cell

quiescence in rat aorta: Role of the cyclin dependent kinases and their inhibitors. *Cardiovasc. Res.* **53**, 242–252
9. Tanner, F. C., Boehm, M., Akyurek, L. M., San, H., Yang, Z. Y., Tashiro, J., Nabel, G. J., and Nabel, E. G. (2000) Differential effects of the cyclin-dependent kinase inhibitors p27(Kip1), p21(Cip1), and p16(Ink4) on vascular smooth muscle cell proliferation. *Circulation* **101**, 2022–2025
10. Nakayama, K. I., and Nakayama, K. (2006) Ubiquitin ligases: Cell-cycle control and cancer. *Nat. Rev. Cancer* **6**, 369–381
11. Carrano, A. C., Eytan, E., Hershko, A., and Pagano, M. (1999) SKP2 is required for ubiquitin-mediated degradation of the CDK inhibitor p27. *Nat. Cell Biol.* **1**, 193–199
12. Bond, M., Sala-Newby, G. B., and Newby, A. C. (2004) Focal adhesion kinase (FAK)-dependent regulation of S-phase kinase-associated protein-2 (Skp-2) stability. A novel mechanism regulating smooth muscle cell proliferation. *J. Biol. Chem.* **279**, 37304–37310
13. Bond, M., Wu, Y. J., Sala-Newby, G. B., and Newby, A. C. (2008) Rho GTPase, Rac1, regulates Skp2 levels, vascular smooth muscle cell proliferation, and intima formation *in vitro* and *in vivo*. *Cardiovasc. Res.* **80**, 290–298
14. Wu, Y. J., Bond, M., Sala-Newby, G. B., and Newby, A. C. (2006) Altered S-phase kinase-associated protein-2 levels are a major mediator of cyclic nucleotide-induced inhibition of vascular smooth muscle cell proliferation. *Circ. Res.* **98**, 1141–1150
15. Wu, Y. J., Sala-Newby, G. B., Shu, K. T., Yeh, H. I., Nakayama, K. I., Nakayama, K., Newby, A. C., and Bond, M. (2009) S-phase kinase-associated protein-2 (Skp2) promotes vascular smooth muscle cell proliferation and neointima formation *in vivo*. *J. Vasc. Surg.* **50**, 1135–1142
16. Demasi, M., and Laurindo, F. R. (2012) Physiological and pathological role of the ubiquitin-proteasome system in the vascular smooth muscle cell. *Cardiovasc. Res.* **95**, 183–193
17. Marciniak, S. J., and Ron, D. (2006) Endoplasmic reticulum stress signaling in disease. *Physiol. Rev.* **86**, 1133–1149
18. Zhang, K., and Kaufman, R. J. (2008) From endoplasmic-reticulum stress to the inflammatory response. *Nature* **454**, 455–462
19. Li, F., Xie, P., Fan, Y., Zhang, H., Zheng, L., Gu, D., Patterson, C., and Li, H. (2009) C terminus of Hsc70-interacting protein promotes smooth muscle cell proliferation and survival through ubiquitin-mediated degradation of FoxO1. *J. Biol. Chem.* **284**, 20090–20098
20. Xie, P., Fan, Y., Zhang, H., Zhang, Y., She, M., Gu, D., Patterson, C., and Li, H. (2009) CHIP represses myocardin-induced smooth muscle cell differentiation via ubiquitin-mediated proteasomal degradation. *Mol. Cell. Biol.* **29**, 2398–2408
21. Lacolley, P., Regnault, V., Nicoletti, A., Li, Z., and Michel, J. B. (2012) The vascular smooth muscle cell in arterial pathology: A cell that can take on multiple roles. *Cardiovasc. Res.* **95**, 194–204
22. Liao, Y., Liu, N., Xia, X., Guo, Z., Li, Y., Jiang, L., Zhou, R., Tang, D., Huang, H., and Liu, J. (2019) USP10 modulates the SKP2/Bcr-Abl axis via stabilizing SKP2 in chronic myeloid leukemia. *Cell Discov.* **5**, 24
23. Takayama, K. I., Suzuki, T., Fujimura, T., Takahashi, S., and Inoue, S. (2018) Association of USP10 with G3BP2 inhibits p53 signaling and contributes to poor outcome in prostate cancer. *Mol. Cancer Res.* **16**, 846–856
24. Wang, X., Xia, S., Li, H., Wang, X., Li, C., Chao, Y., Zhang, L., and Han, C. (2020) The deubiquitinase USP10 regulates KLF4 stability and suppresses lung tumorigenesis. *Cell Death Differ.* **27**, 1747–1764
25. Yuan, J., Luo, K., Zhang, L., Cheville, J. C., and Lou, Z. (2010) USP10 regulates p53 localization and stability by deubiquitinating p53. *Cell* **140**, 384–396
26. Wang, X., Adhikari, N., Li, Q., Guan, Z., and Hall, J. L. (2004) The role of [beta]-transducin repeat-containing protein ([beta]-TrCP) in the regulation of NF-[kappa]B in vascular smooth muscle cells. *Arterioscler. Thromb. Vasc. Biol.* **24**, 85–90
27. Owens, G. K., Kumar, M. S., and Wamhoff, B. R. (2004) Molecular regulation of vascular smooth muscle cell differentiation in development and disease. *Physiol. Rev.* **84**, 767–801
28. Rensen, S. S., Doevendans, P. A., and van Eys, G. J. (2007) Regulation and characteristics of vascular smooth muscle cell phenotypic diversity. *Neth. Heart J.* **15**, 100–108
29. Solway, J., Seltzer, J., Samaha, F. F., Kim, S., Alger, L. E., Niu, Q., Morrisey, E. E., Ip, H. S., and Parmacek, M. S. (1995) Structure and expression of a smooth muscle cell-specific gene, SM22 alpha. *J. Biol. Chem.* **270**, 13460–13469
30. Alexander, M. R., and Owens, G. K. (2012) Epigenetic control of smooth muscle cell differentiation and phenotypic switching in vascular development and disease. *Annu. Rev. Physiol.* **74**, 13–40
31. Gareri, C., De Rosa, S., and Indolfi, C. (2016) MicroRNAs for restenosis and thrombosis after vascular injury. *Circ. Res.* **118**, 1170–1184
32. Shirotani, M., Yui, Y., Hattori, R., and Kawai, C. (1991) U-61,431F, a stable prostacyclin analogue, inhibits the proliferation of bovine vascular smooth muscle cells with little antiproliferative effect on endothelial cells. *Prostaglandins* **41**, 97–110
33. Zohlnhofer, D., Richter, T., Neumann, F., Nuhrenberg, T., Wessely, R., Brandl, R., Murr, A., Klein, C. A., and Baeuerle, P. A. (2001) Transcriptome analysis reveals a role of interferon-gamma in human neointima formation. *Mol. Cell* **7**, 1059–1069
34. Xia, X., Liao, Y., Huang, C., Liu, Y., He, J., Shao, Z., Jiang, L., Dou, Q. P., Liu, J., and Huang, H. (2019) Deubiquitination and stabilization of estrogen receptor alpha by ubiquitin-specific protease 7 promotes breast tumorigenesis. *Cancer Lett.* **465**, 118–128
35. Liao, Y., Guo, Z., Xia, X., Liu, Y., Huang, C., Jiang, L., Wang, X., Liu, J., and Huang, H. (2019) Inhibition of EGFR signaling with Spautin-1 represents a novel therapeutics for prostate cancer. *J. Exp. Clin. Cancer Res.* **38**, 157
36. Liao, Y., Liu, Y., Xia, X., Shao, Z., Huang, C., He, J., Jiang, L., Tang, D., Liu, J., and Huang, H. (2020) Targeting GRP78-dependent AR-V7 protein degradation overcomes castration-resistance in prostate cancer therapy. *Theranostics* **10**, 3366–3381
37. Xia, X., Huang, C., Liao, Y., Liu, Y., He, J., Guo, Z., Jiang, L., Wang, X., Liu, J., and Huang, H. (2019) Inhibition of USP14 enhances the sensitivity of breast cancer to enzalutamide. *J. Exp. Clin. Cancer Res.* **38**, 220
38. Xia, X., Xu, Q., Liu, M., Chen, X., Liu, X., He, J., Hu, T., Yu, C., Huang, H., Liu, S., and Liu, N. (2020) Deubiquitination of CD36 by UCHL1 promotes foam cell formation. *Cell Death Dis.* **11**, 636